A 10-gram Microflyer for Vision-based Indoor Navigation

Jean-Christophe Zufferey*†, Adam Klaptocz*, Antoine Beyeler*, Jean-Daniel Nicoud† and Dario Floreano*
*Laboratory of Intelligent Systems (LIS, http://lis.epfl.ch)
Ecole Polytechnique Fédérale de Lausanne (EPFL, http://www.epfl.ch)
1015 Lausanne, Switzerland
Email: name.surname@epfl.ch
†DIDEL SA (http://www.didel.com)
Chemin de la Mouette 5
1092 Belmont-sur-Lausanne, Switzerland
Email: nicoud@didel.com

***Abstract*— We aim at developing ultralight autonomous microflyers capable of navigating within houses or small built environments. Our latest prototype is a fixed-wing aircraft weighing a mere 10 g, flying around 1.5 m/s and carrying the necessary electronics for airspeed regulation and collision avoidance. This microflyer is equipped with two tiny camera modules, two rate gyroscopes, an anemometer, a small microcontroller, and a Bluetooth radio module. In-flight tests are carried out in a new experimentation room specifically designed for easy changing of surrounding textures.**

I. Challenges and State of the Art

There are currently no autonomous flying robots capable of navigating indoors, within enclosed environments such as offices or houses. Although they could be useful in many applications such as surveillance, hazardous environment exploration, search and rescue, etc., the challenges engineers are facing to develop such robots are numerous. In order to be able to fly at very low speed (below 2 m/s) such flying systems must be ultra-lightweight (usually well below 50 g), which implies tremendous constraints in terms of embedded computational power, sensor simplicity, and airframe architecture. Moreover, controlling such systems is quite different from controlling more conventional outdoor micro aerial vehicles, which can rely on high-precision inertial measurement units, global positioning systems, radars or other conventional distance sensors, and/or visual horizon detection systems [1]–[3].

In this paper we present the latest prototype resulting from our research in the domain of indoor microflyers since 2001 [4]–[7]. This robot, called MC1, has an overall weight of 10 g including visual, inertial, and air flow sensors, which enable a certain degree of autonomy: automatic take-off, speed regulation, and collision avoidance. These capabilities have been demonstrated in a 7x6-m room equipped with randomly textured walls.

To the best of our knowledge, the MC1 is the lightest motorized free-flying robot produced to date. Oh and collaborators have been working on automatic landing and collision avoidance with an indoor flying robot weighing around 30 g [8], [9]. However, these experiments were carried out in relatively large indoor environments such as basketball courts and only one vision sensor was embedded at one time allowing for either controlling altitude or avoiding obstacles on one side only. More recently, Fearing and collaborators developed a remarkable 2-gram microglider [10], but no autonomous operation has been demonstrated so far. Other projects aiming at even smaller flying robots (helicopters [11] or flapping-wings [12], [13]) have been attempted, but no self-powered free flights have been carried out as of yet.

In summer 2004, we demonstrated the first visually-guided free-flying indoor aircraft. This was done with an earlier prototype (designated F2) weighing 30 g and flying in a 16x16-m room equipped with evenly-distributed black and white vertical stripes made of suspended fabrics. The experiment consisted of having the 80-cm-wingspanned aircraft autonomously steer like a fly, i.e., following straight trajectories when far from any walls and engaging a fast left or right turn when close to a wall (see [7] for details).

With the 10-gram MC1 described in this paper, we made three significant steps forward since then:

1) The overall weight of the robot has been reduced from 30 g to 10 g while the maneuverability has been further improved in order to enable experiments in a significantly smaller room: from 256 m^2 to 42 m^2.
2) A new experimentation room equipped with 8 computer-driven projectors has been built, which allows us to demonstrate autonomous flight with more complex visual surroundings than evenly distributed black and white vertical stripes.
3) An ultralight anemometer has been developed in order to automatically regulate the flight velocity.

In the following section, we present the MC1 microflyer, its airframe, electronics, and sensors. We then introduce the proposed control strategy, describe our new experimentation room, and provide some insight on the results obtained so far.

II. Microflyer

A. Airframe and Actuators

The MC1 (Fig. 1) is based on a "microCeline", which is a 5.2-gram home flyer produced by Didel SA (http://www.didel.com) for the hobbyist market. This model is mainly made out of carbon fiber rods and thin Mylar

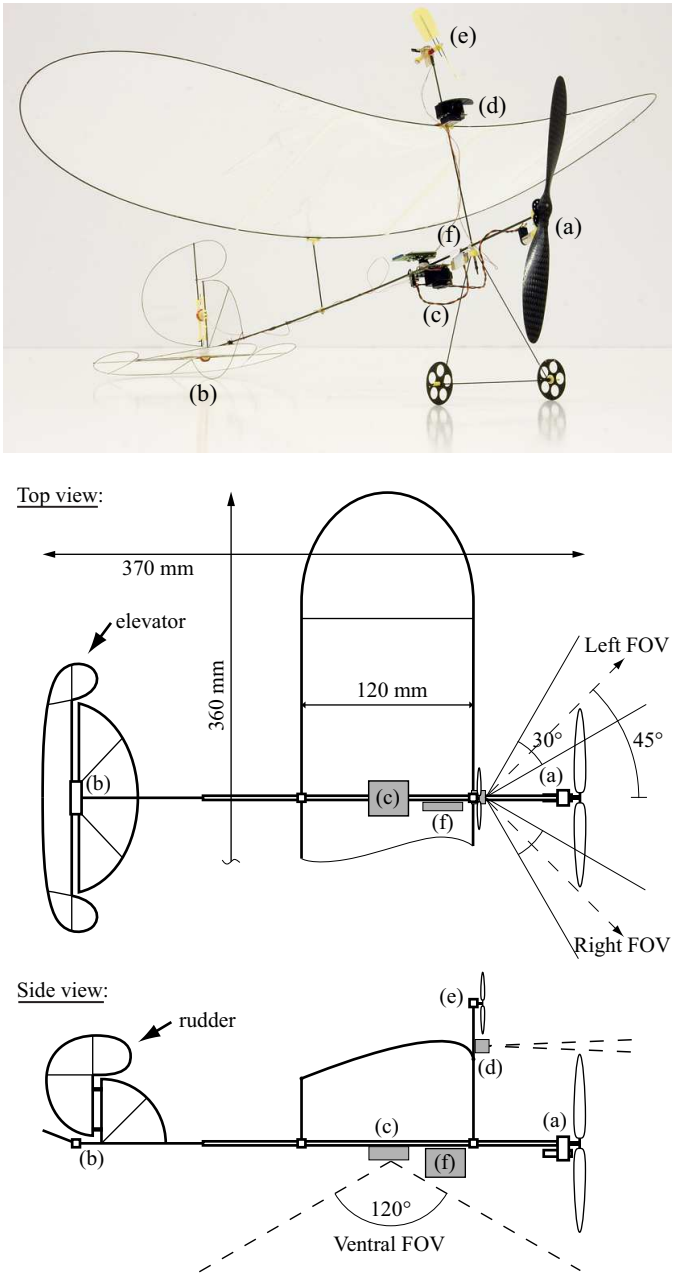

Fig. 1. MC1 microflyer. The on-board electronics consists of (a) a 4mm geared motor with a lightweight carbon fiber propeller, (b) two magnet-in-a-coil actuators controlling the rudder and the elevator, (c) a microcontroller board with a Bluetooth module and a ventral camera with its pitch rate gyro, (d) a front camera with its yaw rate gyro, (e) an anemometer, and (f) a Lithium-polymer battery.

plastic films. The wing and the battery are connected to the frame using small magnets such that they can be easily taken apart. The propulsion is ensured by a 4-mm brushed DC motor, which transmits its torque to a lightweight carbon-fiber propeller via a 1:12 gearbox. The rudder and elevator are actuated by two magnet-in-a-coil actuators. These extremely lightweight actuators are not controlled in position like conventional servos, but because they are driven by bidirectional pulse width modulated (PWM) signals, they are proportional

TABLE I

MASS AND POWER BUDGETS OF THE MC1 MICROFLYER.

Subsystem	Mass [g]	Peak power [mW]
Airframe	1.8	-
Motor, gear, propeller	1.4	800
2 actuators	0.9	450
Lithium-polymer battery	2.0	-
Microcontroller board	1.0	80
Bluetooth radio module	1.0	140
2 cameras with rate gyro	1.8	80
Anemometer	0.4	< 1
Total	10.3	1550

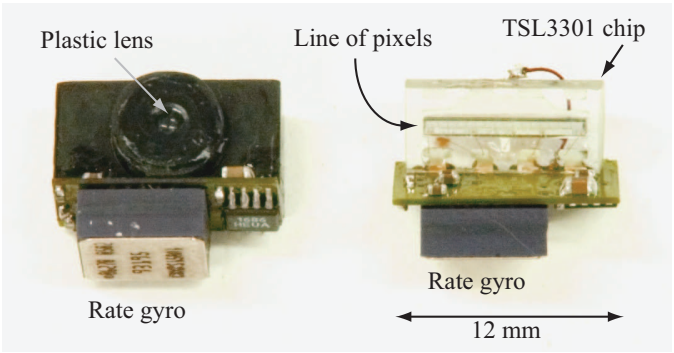

Fig. 2. The 0.9-gram camera module with integrated piezo rate gyro. Left: The entire module, viewed from the lens side, with the rate gyro (Analog Devices, Inc. ADXRS150) soldered underneath the 0.3-mm printed circuit board (PCB). Right: The same module is shown, but without its black plastic cover, in order to highlight the underlying 1D CMOS camera (TAOS, Inc. TSL3301) that has been significantly machined to reduce size and allow vertical soldering on the PCB.

in torque.

At EPFL, we developed the required electronics and control system for autonomous vision-based navigation. When fitted with the sensors and electronics, the total weight of the MC1 reaches 10.3 g (Table I). However, it is still capable of flying in reasonably tight spaces (in the order of 16 m^2) at low velocity (around 1.5 m/s). In this robotic configuration, the average consumption is in the order of 1 W (Table I) and the on-board 65 mAh Lithium-polymer battery ensures an energetic autonomy of slightly more than 10 minutes.

B. Sensors

Since conventional sensors such as radars, lasers, inertial measurement units, and GPS are too heavy and power consuming for such a lightweight robot, we took inspiration from flies, which display impressive flight control capabilities without relying on such sensors. Flies are equipped with large field of view (FOV), low-resolution eyes, two oscillating organs called halteres that provide inertial information similar to rate gyros, and different types of hairs all around the body enabling airflow measurements [14]–[17]. Therefore, we equipped the MC1 with two wide-FOV cameras (though only 1D compared to the 2D image provided by the fly's eyes), two rate gyros for yaw and pitch rotational velocity measurements and an anemometer for airspeed estimation.

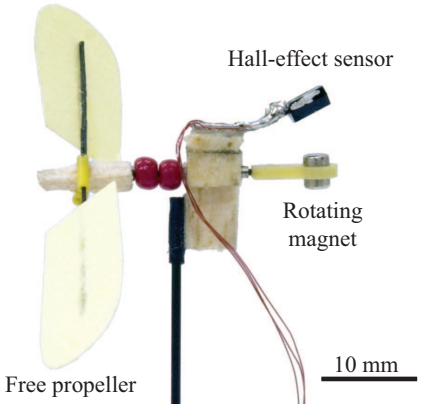

Fig. 3. The 0.4-g anemometer is made of a paper propeller linked to a small magnet that rotates in front of a hall-effect sensor (Allegro3212, SIP package).

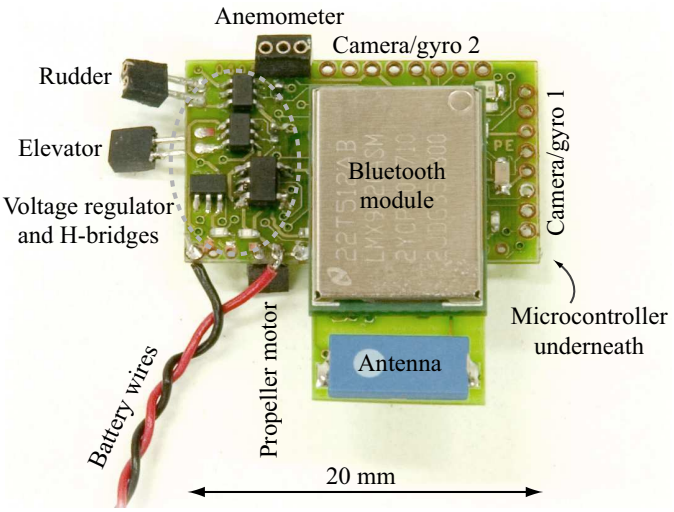

Fig. 4. Microcontroller board (1 g) with Bluetooth module (1 g). The connectors to the various on-board peripherals are indicated on the picture.

As further described in Section III, vision is a prerequisite for computing image velocity - the so-called optic flow (OF) - and together with the gyroscopic information enables rough estimations of distances from surrounding obstacles. Therefore, we developed miniature camera modules each equipped with a piezo rate gyro. In order to fit the limited amount of available computational resources and be capable of acquiring images at high speed (>20 Hz), we selected 1D black-and-white CMOS cameras (Fig. 2) instead of more conventional 2D color cameras that require significantly greater amounts of memory and relatively complex interfaces.

One of these camera modules is oriented forward with its rate gyro measuring yaw rotations, and is meant to be used for steering and obstacle avoidance[1]. The second camera module is oriented downward, looking longitudinally at the ground, while its rate gyro measures rotation about the pitch axis. Each of the cameras have 80 active pixels spanning a total FOV of 120°. In the front camera, only the 20 pixels close to each side of the image are effectively used by the control system at this stage (see Section III for further details).

The MC1 is also equipped with a custom-developed anemometer (Fig. 3) consisting of a free-rotating propeller driving a small magnet in front of a hall-effect sensor in order to estimate airspeed. This anemometer is placed in a region that is not blown by the main propeller. The frequency of the pulsed signal output by the hall-effect sensor is computed by the microcontroller and mapped into an 8-bit variable. This mapping has been experimentally tuned in order to fit the typical values obtained when the MC1 is in flight.

C. Embedded Electronics

The microcontroller board (Fig. 4) is based on a Microchip, Inc. PIC18LF4620 running at 32 MHz with 64 KB of flash program memory and about 4 KB of RAM. The PIC18LF4620 is an 8-bit microcontroller with a reduced instruction set and without floating point arithmetic. However, it has a C-compiler optimized architecture and contains very efficient instructions such as a single-cycle 8-bit multiplication. It has been selected mainly for its low power consumption, internal oscillator, small outline (8x8-mm 44-lead plastic quad flat package), ability to self-program by means of a bootloader using the built-in serial communication port, and its great ability to accommodate a variety of sensors and actuators. It has several configurable PWM outputs and up to 13 A/D converters that are used, for example, to read gyro outputs and battery level. This microcontroller also supports a low voltage (3 V) power supply, which is compatible with the Lithium-polymer battery voltage and the Bluetooth module.

The Bluetooth module is a National Semiconductor, Inc. LMX9820A, which by default enables a virtual serial communication port without any specific drivers running on the host microcontroller. This feature allows us to easily connect to the MC1 from a Bluetooth-enabled laptop to log flight data or reprogram the microcontroller by means of a bootloader (Tiny PIC bootloader, http://www.etc.ugal.ro/cchiculita/software/). The programming process takes a mere 10 s.

III. In-flight Experiments

A. Control Strategy

At this stage, the goal is to enable the MC1 to fly in a textured room, regulate its own airspeed and avoid crashing into the surrounding walls. This is achieved without relying on off-board resources and in a completely autonomous way except for what concerns the altitude, which at the moment is radio-controlled by a human pilot. Note that we are actively investigating vision-based strategies for altitude control using the ventral camera together with the pitch rate gyro and the anemometer [18], but this has not yet been implemented on the MC1.

[1]Note that in previous experiments with the larger airplane [7], we used two 1D cameras for collision avoidance, each one oriented at 45° off the forward direction. The new vision module has a wider FOV so that only one camera is required to span the same regions that were previously covered by these two cameras. This has been made possible by changing the optical diaphragm while using the same low-cost plastic lens.

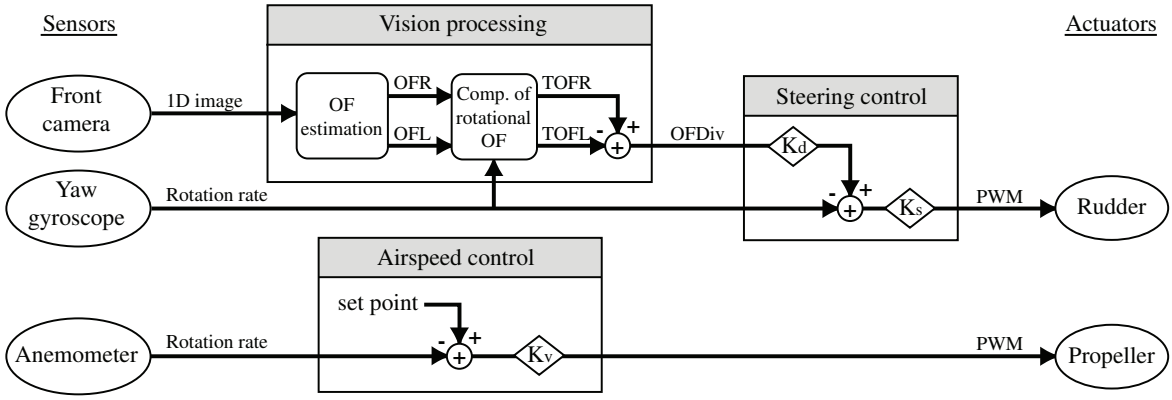

Fig. 5. Control scheme currently implemented on the MC1. Airspeed is regulated by means of a proportional controller with an experimentally tuned anemometer set point and gain labelled Kv. Steering control is based on the yaw rate gyro and OFDiv, which is provided by a vision processing routine (see text for more details). Ks allows to adjust the gain of the steering regulator, whereas Kd is intended for tuning the effect of OFDiv on the steering behaviour and thereby regulating how far the MC1 flies from the surrounding obstacles. The parameters (set point and 3 gains) have been experimentally adjusted.

As shown in Fig. 5 (Airspeed control box), flight speed regulation is achieved by means of a proportional controller taking the anemometer value as input and comparing it against an experimentally determined set point. As a consequence, when the MC1 is at rest on the ground, it will set full power as soon as the controller is started and until a reasonable airspeed (~1.5 m/s) is reached. This will initiate a quick take-off and initial climb until the human pilot pushes on the joystick in order to stop climbing and keep altitude constant. At this point, the MC1 will tend to increase velocity, which will be sensed by the anemometer and result in a decrease of motor power thanks to the airspeed controller feedback.

In order to steer autonomously, the MC1 uses its front camera together with the yaw rate gyro. It is well known that the divergence of optic flow provides a good estimate of the time to contact [19], [20]. This optic flow divergence (OFDiv) can thus be used as a primary cue to sense obstacles and avoid collisions. OFDiv has indeed been shown to play an important role in the fly's turning reaction [21].

As in [7], OF is estimated on the left and right sides of the frontal camera at 45° off the longitudinal axis of the airplane (see Fig. 1, top-view outline) because these are the viewing directions where OF is usually the greatest. The resulting values, obtained by means of an image interpolation algorithm [7], [22], are labelled OFR and OFL for the right and the left part of the FOV, respectively (see Fig. 5, Vision processing box). Since the rotational component of OF induced by rotation of the plane around the yaw axis is not related to distances from surrounding obstacles [23], OFR and OFL are further processed to remove this spurious rotational component using gyroscopic information [7]. The remaining OF values due only to translation (TOFR and TOFL) are then subtracted to provide OFDiv, which is finally used to regulate the turning rate of the MC1 by offsetting the yaw gyro input to a proportional controller connected to the rudder of the plane (see Fig. 5, Steering control box).

B. Experimentation Room

In order to be able to test our indoor microflyers in a large range of controlled environmental conditions, we built a virtual reality arena of 7x6 m in area and 3 m high. The 4 walls are homogeneously painted in white and 8 projectors are hung from the ceiling in order to project any visual texture onto the walls (Fig. 6). Each projector is linked to one of 8 computers, which in turn are inter-connected into a cluster via a 100MB Ethernet network. A custom-made software running on the cluster head drives the nodes to project an image that is adjusted to the exact size of each half wall. The same software can then take a large image as input, cut it into 8 corresponding slices, and send them to each node of the cluster.

C. In-flight Experiments and Results

We present two experiments where the MC1 equipped with the control strategy previously described is started from the ground of our experimentation room and must steer autonomously while regulating its airspeed. The only difference between experiments is the type of projected texture. In the first experiment, randomly distributed black and white stripes are used, whereas in the second one a black and white checkerboard pattern is projected (Fig. 7). This latter texture is more difficult for OF estimation since roll movements of the plane can dramatically change the visual content from one image acquisition to the next. However, at this preliminary stage, the goal of these two experiments is not to systematically investigate effects of different visual textures or control parameters, but rather to demonstrate autonomous operation of the MC1 as a proof-of-concept. A video clip corresponding to these experiments is available in the video proceedings of the conference and for download from the project website (http://lis.epfl.ch/microflyers).

These experiments were carried out several times with the same control strategy and the MC1 demonstrated good robustness with both kinds of visual textures meaning that it could fly for up to 10 minutes without crashing. Fig. 7 shows a subset of flight data recorded during the first 25 s of the

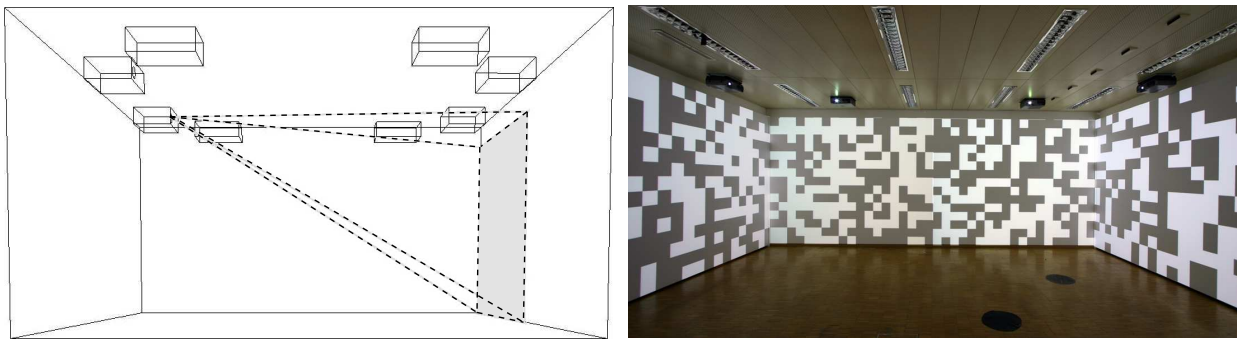

Fig. 6. Our 7x6-m experimentation room for indoor aerial vision-based navigation. Left: Arrangement of the 8 projectors hanging from the ceiling, each projecting on the opposite half-wall. Note the dashed pyramidal outline showing as an example the zone illuminated by the left-back projector. Right: Picture of the interior of this room with a random checkerboard pattern being projected.

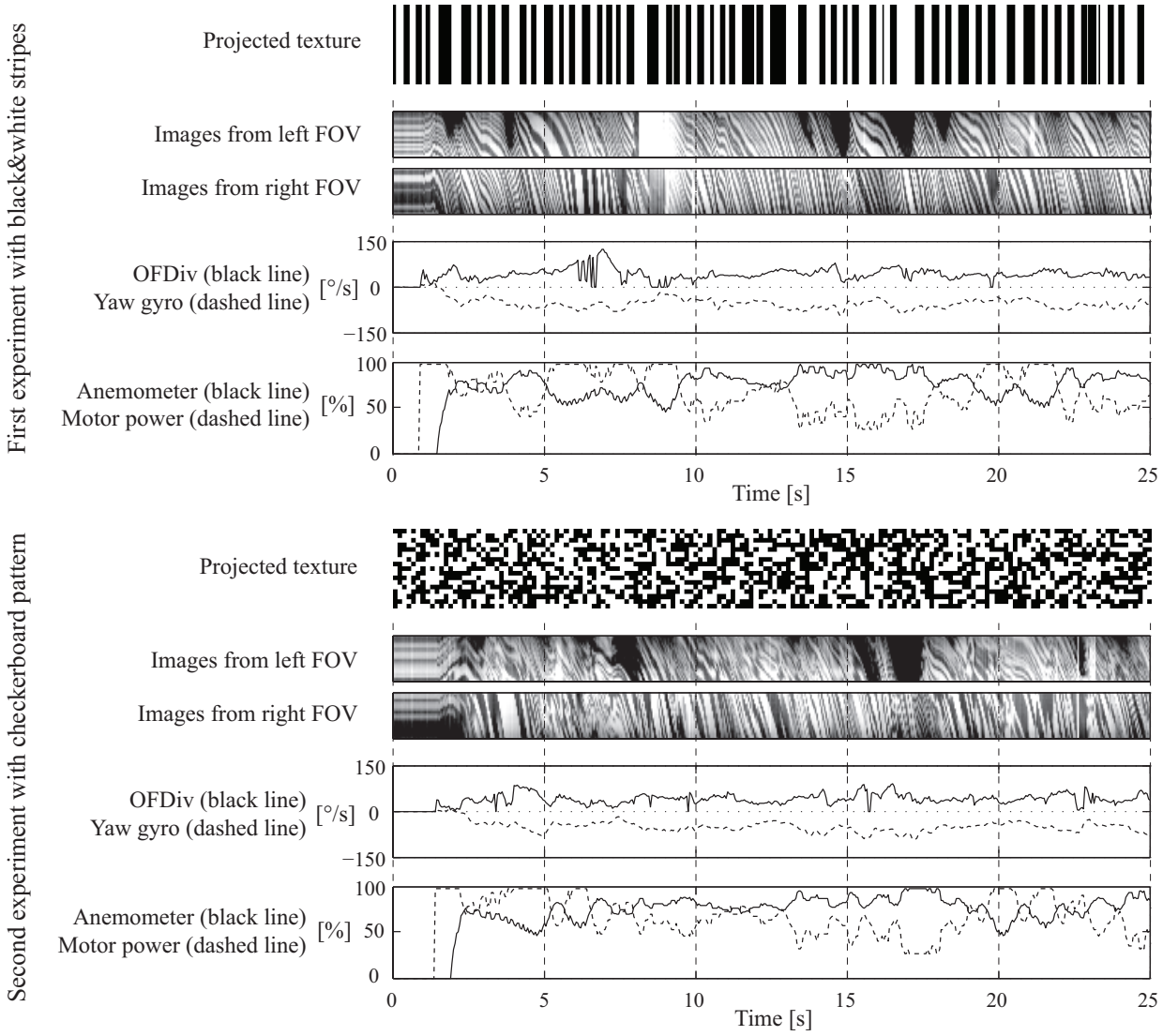

Fig. 7. 25-second extract of flight data from two experiments. For each experiment, the first line represents the texture projected in the experimentation room: randomly sized black and white stripes for the first one, and random checkerboard pattern for the second one (same as in Fig. 6, right). The second line shows the images (in this graph, images have been rotated vertically) taken over time by the front camera in the two regions where OF is estimated, i.e., 1 line of 20 pixels for each side corresponding to the left FOV and the right FOV indicated in Fig. 1. The third line gives the evolution over time of the OF divergence (dependent on the distance from the surrounding walls) and the yaw gyro providing an idea of how much the MC1 is turning. The fourth line shows the evolution of the anemometer value together with the motor setting. Flight data are sampled every 50ms, which correspond to the sensory-motor cycle duration.

flight when the robot takes off, climbs, and levels off. During those 25 s, the MC1 travels approximately 4 times around the room.

The bottom graphs of each experiment (Fig. 7) show the motor power settings and anemometer values over time. At the beginning, one can easily distinguish when autonomous control is initiated since it corresponds to the moment when the motor power rises from 0% to 100%. The anemometer then reacts to the plane's acceleration, and after one or two seconds the plane has reached its cruising altitude and the human pilot levels it off with a slight push on the joystick. The motor power is then continuously adapted according to the anemometer value.

Fig. 7 also shows the signals related to steering control, i.e., OFDiv and yaw rate gyro. A quick inspection of the gyro signal indicates that the MC1 is flying in leftward circles and continuously adapts its turning rate according to OFDiv. A closer look at those signals reveals the direct, though slightly delayed, impact of OFDiv on the turning rate of the plane.

By looking at the raw images taken by the front camera (Fig. 7), one can see that image quality is not always perfect. For instance, blackouts occur quite often on the left side while the plane is banking leftward. This is because the opposite wall is far away and some pixels aim at the ground. Whiteouts also occur occasionally when the camera happens to be directed at a projector. In those particular cases where image contrast is significantly low, OF is set to zero and no compensation for rotational OF is done. In the right FOV however, images are generally of good quality since the wall is closer. In spite of the poor image quality resulting in a noisy OFDiv signal, the overall behaviour of the plane is robust and almost independent of the kind of visual texture (vertical stripes or checkerboard).

IV. Conclusion and Outlook

This paper describes a proof-of-concept 10-gram microflyer steering autonomously in a textured indoor environment. This has been achieved using fly-inspired sensors and control strategy. Those results go well beyond previous experiments [7] in that the microflyer is 3 times lighter (even though it has increased field of view and additional sensors), flies in an experimentation room 6 times smaller with more complex visual textures, and is capable of regulating its own airspeed by means of a small anemometer.

In the future, we plan to investigate more systematically the impact of modifying control parameters and visual textures. In order to be able to precisely characterise the obtained behaviours, we are currently developing a vision-based 3D tracking system. Altitude control will also be implemented at some point. All these developments are intended to pave the way toward fully autonomous flight in natural indoor environments.

Acknowledgment

The authors wish to thank André Guignard for his expert support in miniature camera design and construction. This project is supported by the Swiss National Science Foundation, grant number 200021-105545/1.

References

[1] T. Mueller, *Fixed and Flapping Wing Aerodynamics for Micro Air Vehicle Applications*, vol. 195 of *Progress in Astronautics and Aeronautics*. AIAA, 2001.

[2] J. Grasmeyer and M. Keennon, "Development of the black widow micro air vehicle," in *Fixed and Flapping Wing Aerodynamics for Micro Air Vehicle Applications* (T. J. Mueller, ed.), vol. 195 of *Progress in Astronautics and Aeronautics*, pp. 519–535, AIAA, 2001.

[3] S. Ettinger, M. Nechyba, P. Ifju, and M. Waszak, "Vision-guided flight stability and control for micro air vehicles," *Advanced Robotics*, vol. 17, no. 3, pp. 617–40, 2003.

[4] J. Nicoud and J.-C. Zufferey, "Toward indoor flying robots," in *IEEE/RSJ International Conference on Intelligent Robots and Systems*, pp. 787–792, 2002.

[5] J.-C. Zufferey and D. Floreano, "Toward 30-gram autonomous indoor aircraft: Vision-based obstacle avoidance and altitude control," in *Proceedings of the IEEE International Conference on Robotics and Automation, Barcelona*, 2005.

[6] J.-C. Zufferey, *Bio-inspired Vision-based Flying Robots*. PhD thesis, Swiss Federal Institute of Technology in Lausanne (EPFL), 2005.

[7] J.-C. Zufferey and D. Floreano, "Fly-inspired visual steering of an ultralight indoor aircraft," *IEEE Transactions on Robotics*, vol. 22, no. 1, pp. 137–146, 2006.

[8] W. Green, P. Oh, K. Sevcik, and G. Barrows, "Autonomous landing for indoor flying robots using optic flow," in *ASME International Mechanical Engineering Congress and Exposition*, vol. 2, pp. 1347–1352, 2003.

[9] W. Green, P. Oh, and G. Barrows, "Flying insect inspired vision for autonomous aerial robot maneuvers in near-earth environments," in *Proceeding of the IEEE International Conference on Robotics and Automation*, 2004.

[10] R. Wood, S. Avadhanula, E. Steltz, M. Seeman, J. Entwistle, A. Bachrach, G. Barrows, S. Sanders, and R. Fearing, "Design, fabrication and initial results of a 2g autonomous glider," in *IEEE Industrial Electronics Society 2005 Meeting, Raleigh North Carolina*, 2005.

[11] I. Kroo and P. Kunz, "Mesoscale flight and miniature rotorcraft development," in *Fixed and Flapping Wing Aerodynamics for Micro Air Vehicle Applications* (T. J. Mueller, ed.), vol. 195 of *Progress in Astronautics and Aeronautics*, pp. 503–517, AIAA, 2001.

[12] R. Fearing, K. Chiang, M. Dickinson, D. Pick, M. Sitti, and J. Yan, "Wing transmission for a micromechanical flying insect," in *Proceeding of the IEEE International Conference on Robotics and Automation*, pp. 1509–1516, 2000.

[13] S. Avadhanula, R. Wood, E. Steltz, J. Yan, and R. Fearing, "Lift force improvements for the micromechanical flying insect," in *Proceeding of the IEEE Int. Conf. on Intelligent Robots and Systems*, 2003.

[14] M. Land, "Visual acuity in insects," *Annual Review of Entomology*, vol. 42, pp. 147–177, 1997.

[15] G. Nalbach, "The halteres of the blowfly calliphora. I. Kinematics and dynamics," *Journal of Comparative Physiology A*, vol. 173, no. 3, pp. 293–300, 1993.

[16] R. Chapman, *The Insects: Structure and Function*. Cambridge University Press, 4th ed., 1998.

[17] R. Dudley, *The Biomechanics of Insect Flight: Form, Function, Evolution*. Princeton University Press, 2000.

[18] A. Beyeler, C. Mattiussi, J.-C. Zufferey, and D. Floreano, "Vision-based altitude and pitch estimation for ultra-light indoor aircraft," in *IEEE International Conference on Robotics and Automation ICRA '06*, pp. 2836–2841, 2006.

[19] N. Ancona and T. Poggio, "Optical flow from 1D correlation: Application to a simple time-to-crash detector," in *Proceedings of Fourth International Conference on Computer Vision*, pp. 209–214, 1993.

[20] D. Lee, "A theory of visual control of braking based on information about time-to-collision," *Perception*, vol. 5, pp. 437–459, 1976.

[21] L. Tammero and M. Dickinson, "The influence of visual landscape on the free flight behavior of the fruit fly drosophila melanogaster," *The Journal of Experimental Biology*, vol. 205, pp. 327–343, 2002.

[22] M. Srinivasan, "An image-interpolation technique for the computation of optic flow and egomotion," *Biological Cybernetics*, vol. 71, pp. 401–416, 1994.

[23] J. Koenderink and A. van Doorn, "Facts on optic flow," *Biological Cybernetics*, vol. 56, pp. 247–254, 1987.